ARTICLE
Journal of Cellular Biochemistry 114:1940–1954 (2013)

Journal of Cellular Biochemistry

Mechanisms of Ceramide-Induced COX-2-Dependent Apoptosis in Human Ovarian Cancer OVCAR-3 Cells Partially Overlapped With Resveratrol

Hung-Yun Lin,[1]* Dominique Delmas,[2,3] Ole Vang,[4] Tze-Chen Hsieh,[5] Sharon Lin,[6] Guei-Yun Cheng,[1] Hsiao-Ling Chiang,[1] Chiao En Chen,[1] Heng-Yuan Tang,[6] Dana R. Crawford,[7] Jacqueline Whang-Peng,[1] Jaulang Hwang,[8] Leroy F. Liu,[1,9] and Joseph M. Wu[5]

[1]*Institute of Cancer Biology and Drug Discovery, Taipei Medical University, Taipei, Taiwan*
[2]*Université de Bourgogne, Faculté de Médecine, Dijon, Bourgogne, France*
[3]*INSERM U866 "Chemotherapy, Lipid Metabolism and Antitumoral Immune Response", Dijon, Bourgogne, France*
[4]*Department of Science, Systems and Models, Roskilde University, Roskilde, Denmark*
[5]*Department of Biochemistry and Molecular Biology, New York Medical College, Valhalla, New York*
[6]*Pharmaceutical Research Institute, Albany College of Pharmacy and Health Sciences, Albany, New York*
[7]*Center for Immunology & Microbial Disease, Albany Medical College, Albany, New York*
[8]*Department of Biochemistry, School of Medicine, Taipei Medical University, Taipei, Taiwan*
[9]*Department of Pharmacology, University of Medicine and Dentistry of New Jersey-Robert Wood Johnson Medical School, Piscataway, New Jersey*

ABSTRACT

Ceramide is a member of the sphingolipid family of bioactive molecules demonstrated to have profound, diverse biological activities. Ceramide is a potential chemotherapeutic agent via the induction of apoptosis. Exposure to ceramide activates extracellular-signal-regulated kinases (ERK) 1/2- and p38 kinase-dependent apoptosis in human ovarian cancer OVCAR-3 cells, concomitant with an increase in the expression of COX-2 and p53 phosphorylation. Blockade of cyclooxygenase-2 (COX-2) activity by *siRNA* or NS398 correspondingly inhibited ceramide-induced p53 Ser-15 phosphorylation and apoptosis; thus COX-2 appears at the apex of the p38 kinase-mediated signaling cascade induced by ceramide. Induction of apoptosis by ceramide or resveratrol was inhibited by the endocytosis inhibitor, cytochalasin D (CytD); however, cells exposed to resveratrol showed greater sensitivity than ceramide-treated cells. Ceramide-treated cells underwent a dose-dependent reduction in trans-membrane potential. Although both ceramide and resveratrol induced the expressions of caspase-3 and -7, the effect of inducible COX-2 was different in caspase-7 expression induced by ceramide compared to resveratrol. In summary, resveratrol and ceramide converge on an endocytosis-requiring, ERK1/2-dependent signal transduction pathway and induction of COX-expression as an essential molecular antecedent for subsequent p53-dependent apoptosis. In addition, expressions of caspase-3 and -7 are observed. However, a p38 kinase-dependent signal transduction pathway and change in mitochondrial potential are also involved in ceramide-induced apoptosis. J. Cell. Biochem. 114: 1940–1954, 2013.

KEY WORDS: CERAMIDE; RESVERATROL; COX-2; p53; p38 KINASE; APOPTOSIS

Disclosure statement: Dr. Ole Vang is the consultant for Fluxome A/S; none of the other authors have a financial interest in the subject of this article.

*Correspondence to: Hung-Yun Lin, Institute of Cancer Biology and Drug Discovery, Taipei Medical University, 250 Wu-Hsing Street, Taipei, Taiwan. E-mail: linhy@tmu.edu.tw

Manuscript Received: 29 March 2012; Manuscript Accepted: 28 February 2013
Accepted manuscript online in Wiley Online Library (wileyonlinelibrary.com): 13 March 2013
DOI 10.1002/jcb.24539 • © 2013 Wiley Periodicals, Inc.

In the United States, epithelial ovarian cancer is still currently considered the leading gynecologic cause of cancer death despite significant advances in chemotherapy and combination drug treatment modalities [Bhoola and Hoskins, 2006]. A diagnosis is usually made at late stages of the disease, making complete surgical resection challenging and difficult to achieve [Morrison et al., 2007].

Ceramides are structurally and functionally heterogeneous molecules belonging to the sphingolipid family that are found in abundance on cell membranes [Hannun and Obeid, 2011]. Ceramides can be generated by hydrolysis of sphingomyelin or via de novo synthesis in response to physiological stimuli such as tumor necrosis factor-α, interferon-γ, and interleukins or upon exposure to pharmacological agents including anticancer drugs, notably, daunorubicin, vincristine, 1α-D-arabinofuranosylcytosine, and retinoids [Hannun and Linardic, 1993; Oskouian and Saba, 2010]. Ceramides have been reported to induce apoptosis, in part due to their ability to produce a collapse of the mitochondrial membrane electrochemical potential, consequently increasing mitochondrial permeability [Cianchi et al., 2006]. Conceivably, additional mechanisms might be involved in their apoptotic activities in responsive cells. Owing to their membrane permeability property, short-chain ceramides have been tested in early clinical trials as an anti-breast cancer agent [Perry and Kolesnick, 2003]. Notwithstanding, many details concerning their anti-carcinogenic activities remain unexplored.

We are interested in examining the mechanisms and signal transduction pathways involved in the induction of apoptosis mediated by ceramide. We focused our analysis on COX-2, which has been reported to exhibit anti-proliferative activities independent of the synthesis of prostaglandin PGE2 [Trifan et al., 1999] but appears to require the induction of the tumor suppressor protein, p53, as well as p21 [Zahner et al., 2002]. The ability of p53 to induce COX-2 expression during genotoxic stress-induced apoptosis further illustrates the complex relationship between COX-2 and cell proliferation [Corcoran et al., 2005]. Resveratrol (*trans*-3,4',5-trihydroxystilbene) is a naturally occurring polyphenolic compound highly enriched in grapes, peanuts, red wine, and a variety of food sources. Resveratrol has been reported to elicit many cellular responses including cell cycle arrest, differentiation, and apoptosis [Aggarwal et al., 2000; Lin et al., 2011a]. Resveratrol can also function as an anti-oxidant and reduces the risk of developing coronary heart disease [Das et al., 1999]. A cell surface receptor for the stilbene is identified on integrin αvβ3 [Lin et al., 2006] and is shown to be linked to activation of the MAPK signal transduction pathway [Lin et al., 2006]. Resveratrol has been shown to activate a ceramide-dependent signal transduction pathway [Scarlatti et al., 2003] and likewise acts as a cancer chemopreventive agent by inducing apoptosis in various cancer cell lines; and because our previous studies have shown that nuclear accumulation of COX-2, in response to treatment by resveratrol facilitates p53-dependent apoptosis in human breast cancer [Tang et al., 2006], glioma [Lin et al., 2008a], head-and-neck cancer [Lin et al., 2008b], and ovarian cancer cells [Lin et al., 2011a]. Therefore, we tested whether ceramide and resveratrol may elicit similar or identical molecular activities and cellular events.

In this study, we found that: (1) activation of ERK1/2 kinases and p38 kinase is essential for ceramide-induced COX-2 expression and apoptosis, (2) endocytosis, occurring by an integrin αvβ3-independent mechanism, is required for ceramide-induced apoptosis. Additionally, when mechanisms of signal transduction and apoptosis were compared with those involved in resveratrol-induced apoptosis, we observed that ceramide activates mitochondrial potential but both ceramide and resveratrol induced expression of caspase-3 and caspase-7. Garnering evidence that resveratrol and ceramide display partially overlapping signaling pathways and mechanisms suggests they have potential to be used in sequence or in combination, as novel anti-apoptotic agents beyond what is currently understood.

MATERIALS AND METHODS

CELL LINE

The human ovarian cancer cell line, OVCAR-3, was purchased from American Type Culture Collection (ATCC). Cells were maintained for study in RPMI-1640 (Invitrogen) supplemented with 20% FBS (Sigma-Aldrich, St. Louis, MO) and insulin (Sigma-Aldrich), in a 5% CO_2/95% O_2 incubator at 37°C. Prior to treatment, cells were re-fed with 0.25% stripped FBS-containing medium for 2 days to synchronize cells.

REAGENTS AND ANTIBODIES

RGD (arginine–glycine–aspartic acid) and RGE (arginine–glycine–glutamic acid) peptides and resveratrol were purchased from Sigma-Aldrich. Ceramide, ERK1/2 inhibitor (PD98059), p38 kinase inhibitor (SB203580) and p53 inhibitor (pifithrin-α, PFT-α) were obtained from Calbiochem (Billerica, MA). COX-2 inhibitor (NS398) was obtained from Cayman Chemical (Ann Arbor, MI). Non-specific COX-1/COX-2 inhibitor, indomethacin, was obtained from Sigma-Aldrich. Polyclonal rabbit anti-phosphoMAPK (anti-pERK1/pERK2) and anti-phospho-Ser-15 p53 antibodies were purchased from Cell Signaling (Danvers, MA). Monoclonal mouse anti-BcL-x, polyclonal anti-β-actin, and anti-lamin B were purchased from Santa Cruz Biotechnology (Santa Cruz, CA). Polyclonal rabbit anti-Bcl-x-s antibody was purchased from Biorbyt (San Francisco, CA). Monoclonal mouse anti-human COX-2 and anti-human COX-1 antibodies were purchased from Cayman Chemical. Goat anti-rabbit IgG and rabbit anti-mouse IgG were purchased from Dako (Carpinteria, CA). Chemiluminescence reagents were obtained from Pierce (Rockford, IL). RNeasy® Plus Mini Kit and PCR reaction reagents were obtained from Qiagen (Valencia, CA). RT and qPCR reagents were obtained from Quanta Biosciences (Gaithersburg, MD). siRNA, scRNA, transfection reagent, and primers were obtained from Santa Cruz Biotechnology. Chromatin Immunoprecipitation kit, EZ ChIP kit was purchased from Millipore (Billerica, MA). Cell death detection ELISA Plus assay kit was obtained from Roche Diagnostics (Indianapolis, ID). Caspase-3 activity kit was purchased from Promega (Fitchburg, WI).

CELL FRACTIONATION

Fractionation in a microfuge and preparation of nucleoproteins was conducted according to our previously reported methods [Lin et al., 1999a,b, 2005, 2009; Davis et al., 2000, 2006]. Nuclear extracts were prepared by resuspension of the crude nuclei in high salt buffer (hypotonic buffer containing 420 mM NaCl and 20% glycerol)

at 4°C with rocking for 1 h. The supernatants were collected after subsequent centrifugation at 4°C and 13,000 rpm for 10 min.

IMMUNOBLOTTING

Standard techniques were used and have been previously described in our other publications [Davis et al., 2000, 2006; Lin et al., 1999a,b, 2005, 2009]. In brief, proteins were separated on discontinuous SDS–PAGE (10% or 14% gels) and then transferred by electroblotting to nitrocellulose membranes (Millipore). After blocking with 5% milk in Tris-buffered saline containing 0.1% Tween-20, the membranes were incubated with various antibodies overnight. Secondary antibodies were either goat anti-rabbit IgG (1:1,000) (Dako) or rabbit anti-mouse IgG (1:1,000) (Dako), depending upon the source of the primary antibody. Immunoreactive proteins were detected by chemiluminescence.

INDUCTION OF APOPTOSIS/NUCLEOSOMES

Cells were seeded in 100 mm culture dishes. After ceramide treatment for 48 h, cells were harvested and washed twice with PBS. Nucleosome ELISA assays were carried out according to the protocol provided by Calbiochem. The detailed methodology has been described previously [Lin et al., 2008b, 2011a].

DNA FRAGMENTATION ASSAY

DNA fragmentation assay was performed using a Cell Death Detection ELISA Plus Assay Kit (Roche Diagnostics). Briefly, 20 µl aliquots of supernatant obtained from cell lysates were dispensed to streptavidin-coated 96-well microliter plates followed by addition of 80 µl of antibody cocktail. Plates were incubated for 2 h at room temperature with mild shaking. The antibody cocktail consisted of a mixture of anti-histone biotin and anti-DNA-HRP directed against various histones and antibodies to both single-strand DNA and double-strand DNA, which are major constituents of the nucleosomes. After incubation, unbound components were removed by washing with the incubation buffer. Quantitative determination of the amount of nucleosomes retained by anti-DNA-HRP in the immunocomplex was conducted spectrophotometrically with ABTS as an HRP substrate. Measurements were made at 405 nm against an ABTS solution as a blank (reference wavelength 490 nm) using a Biotekmicroplate reader.

MEASUREMENT OF CASPASE-3 ACTIVITY

Caspase-3 activity was used as an early marker of apoptosis and measured using a synthetic substrate, Ac-DEVD-MCA, according to the method provide by manufactory as described in published literatures [Anantharam et al., 2002]. After treatment with ceramide or resveratrol, cells were washed with PBS, resuspended in lysis buffer containing 50 mM Tris/HCl (pH 7.4), 1 mM EDTA, 10 mM EGTA, and 10 µM digitonin, and incubated at 37°C for 20 min. The lysates were centrifuged at 5,000*g* for 5 min in an Eppendorf centrifuge 5415 C. The supernatants were incubated with the fluorometric caspase-3 substrate, 50 µM Ac-DEVD-AFC, at 37°C for 1 h. Formation of 7-amido-4-trifluoromethylcoumarin (AFC) resulting from caspase cleavage was measured using a fluorescence plate reader (excitation 400 nm, emission 505 nm). All the fluorescence signals from the samples were normalized to protein concentration, as determined with the Bio-Rad Protein Assay.

TRANSFECTION OF siRNA

This methodology was as described previously [Tang et al., 2006]. OVCAR-3 cells were seeded onto 6-well tissue culture plates at 60–80% confluence and in the absence of antibiotic for 24 h before transfection. Immediately prior to transfection, the culture medium was removed and the cells washed once with PBS, then transfected with either scrambled RNA (*scRNA*) or small interfering RNA (*siRNA*) (0.2 µg/well), using Oligofectamine (2 µg/well) in Opti-MEM I medium according to the manufacturer's instructions (Ambion, Austin, TX). The small interfering *RNA* (*siRNA*) of COX-2 and scrambled RNA (*scRNA*) were purchased from Ambion. After transfection, cultures were incubated at 37°C for 4 h and then placed in fresh culture medium. At 24 h after transfection, the medium was removed and replaced with RPMI 1640 with 20% FBS medium. After an additional 48 h, cells were utilized for experimentation.

CHROMATIN IMMUNOPRECIPITATION AND QUANTITATIVE PCR

After treatment with either 20 µM ceramide or 20 µM resveratrol for 48 h, a total of 6×10^6 cells were exposed to 1% formaldehyde for 15 min at room temperature to effect crosslinking [Tang et al., 2004, 2006; Lin et al., 2009]. ChIP was performed using the EZ ChIP kit (Millipore) according to the manufacturer's instructions. Formaldehyde was directly added to the medium (final concentration 1%) for 10 min to crosslink nuclear proteins with genomic DNA. Then 1.25 M glycine was added for 5 min to each dish to quench unreacted formaldehyde. Cells were washed twice in PBS before being scraped in 1 ml PBS with protease inhibitors (PI) (Complete Mini protease inhibitor cocktail tablets, Roche Diagnostics). Cells were centrifuged for 5 min at 700*g* and re-suspended in 1 ml of SDS lysis buffer (1% SDS, 10 mM EDTA, 50 mM Tris, pH 8.1) containing PI. After brief sonication, the resulting supernatant contained DNA fragments ranging from 200 to 1,000 bp. Samples were diluted (1:10) in ChIP dilution buffer (16.7 mM Tris–HCl, pH 8.1; 0.01% SDS; 1.1% Triton X-100, 167 mM NaCl, and 1.2 mM EDTA) containing PI. Samples were pre-cleared with a Protein G Agarose/salmon sperm DNA slurry for 1 h at 4°C. The agarose was pelleted and supernatant was removed with 10 µl set aside as Input. Supernatant was then allowed to incubate overnight at 4°C with mouse anti-COX-2 antibody (Cayman Chemical). Fifty microliters of Dynabeads Protein G (Invitrogen) were added for 1 h at 4°C with rotation. DNA–protein complexes were recovered from beads by washing with Low Salt Immune Complex Wash Buffer (0.1% SDS, 1% Triton X-100, 2 mM EDTA, 20 mM Tris–HCl, pH 8.1, 150 mM NaCl), High Salt Immune Complex Wash Buffer (0.1% SDS, 1% Triton X-100, 2 mM EDTA, 20 mM Tris–HCl, pH 8.1, 500 mM NaCl), LiCl Immune Complex Wash Buffer (0.25 M LiCl, 1% IGEPAL-CA630, 1% deoxycholic acid, 1 mM EDTA, 10 mM Tris, pH 8.1) (one wash each) and two washes using TE Buffer (10 mM Tris–HCl, 1 mM EDTA, pH 6.0). Samples were eluted twice with 100 µl elution buffer (20 µl 10% SDS, 20 µl 1 M $NaHCO_3$ and 160 µl sterile water). To reverse crosslinking, samples were incubated at 65°C for 6 h or overnight with 8 µl 5 M NaCl. One microliter of RNase A was added for 30 min at 37°C before incubating at 45°C for 1–2 h with 4 µl 0.5 M EDTA, 8 µl 1 M Tris–HCl, and 1 µl Proteinase K. DNA was then purified using a Qiagen PCR Purification Kit. Samples were then analyzed by qPCR. Five microliters of DNA were combined with 10 µl of Perfecta SYBR Green Fast Mix (Quanta Biosciences), 0.3 µl each of 20 µM

forward and reverse primers, and 4.7 µl DNase/RNase free water in a MicroAmp™ Optical 384-Well Reaction Plate (Applied Biosystems). The reactions were performed in an ABI Prism 7900 HT SDS instrument (Applied Biosystems) using the following conditions: 2 min at 50°C, 10 min at 95°C, 40 cycles of 15 sec at 95°C, and 1 min at 60°C. Data were analyzed with the 7900 HT Sequence Detection Systems Software (version 2.2.3, Applied Biosystems).

RT-PCR

Total RNA was isolated as described previously [Tang et al., 2004, 2006; Lin et al., 2009]. First-strand cDNA templates were amplified for mRNAs by polymerase chain reaction (PCR) using Taq PCR Master Mix kit (Qiagen). The PCR cycle was an initial step of 95°C for 3 min, followed by 94°C for 1 min, 55°C for 1 min, 72°C for 1 min, then 25 cycles and a final cycle of 72°C for 8 min. PCR products were separated by electrophoresis on 2% agarose gels containing 0.2 µg of ethidium bromide/ml. Gels were visualized under UV light and photographed with Versadoc (Bio-Rad). The resulting images were scanned under direct light for quantitation and documentation. Results from PCR products of specific genes were normalized to the GAPDH signal.

QUANTITATIVE REAL-TIME PCR

Total RNA was extracted using the RNeasy® Plus Mini Kit (Qiagen) and cDNA was synthesized using qScript™ cDNA SuperMix (Quanta Biosciences). Quantitative PCR was conducted with 5 µl of DNA combined with 10 µl of Perfecta SYBR Green FastMix (Quanta Biosciences), 0.3 µl each of 20 µM forward and reverse primers, and 4.7 µl DNase/RNase free water in a MicroAmp™ Optical 384-Well Reaction Plate (Applied Biosystems). The sequences for the primers amplified are listed in Table I. The reactions were performed in an ABI Prism 7900 HT SDS instrument (Applied Biosystems) using the following conditions: 2 min at 50°C, 10 min at 95°C, 40 cycles of 15 sec at 95°C, and 1 min at 60°C. Data were analyzed with the 7900 HT Sequence Detection Systems Software (version 2.2.3, Applied Biosystems). Samples were amplified in triplicate, and data were normalized with expression of β-actin.

DETECTION OF LOSS OF MITOCHONDRIAL TRANS-MEMBRANE POTENTIAL

The change in mitochondrial trans-membrane potential that was occurring during apoptosis was detected by a fluorescence-based assay. The OVCAR-3 cells were cultured as previously described. After being starved with 0.25% stripped FBS-containing medium for 2 days, the cells were re-fed using 20% stripped FBS-containing medium and treated with an appropriate amount of either resveratrol or ceramide. After 24 h, the cells were processed using the JC-1 Mitochondrial Membrane Potential Assay kit (Cayman Chemical), according to the manufacturer's instructions. Approximately 1×10^6 cells were pelleted from each sample and resuspended using 1 ml diluted JC-1 Reagent before being incubated for 30 min in a 37°C, 5% CO_2 incubator. Cells were then analyzed using flow cytometry with a BD™ LSR II (BD Biosciences), using BD FACSDiva™ software.

DATA ANALYSIS AND STATISTICS

Immunoblot and nucleotide densities were measured with a Storm 860 phosphorimager, followed by analysis with ImageQuant software (Molecular Dynamics). Student's *t*-test, with $P < 0.05$ as the threshold for significance, was used to evaluate the significance of the agents and inhibitor effects.

TABLE I. Primer Sequences

Primer	Sequences 5'–3'
ChIP promoters	
β-actin	Forward: AGAAAATCTGGCACCACACC
	Reverse: GGGGTGTTGAAGGTCTCAAA
PIG3	Forward: CAGGACTGTCAGGAGGAGGCGAGTGATAAGG
	Reverse: GTGCGATTCTAGCTCTCACTTCAAGGAGAGG
RT-PCR	
BAD	Forward: GTTTGAGCCGAGTGAGCAGG
	Reverse: ATAGCGCTGTGCTGCCCAGA
Caspase 3	Forward: TTAATAAAGGTATCCATGGAGAACACT
	Reverse: TTAGTGATAAAAATAGAGTTCTTTTGTGAG
Caspase 7	Forward: ATGGCAGATGATCACGGCTGTATTG
	Reverse: TATAGACAATCACGTCAAAACCCA
COX-2	Forward: TTCAAATGAGATTGTGGGAAAATTGCT
	Reverse: AGATCATCTCTGCCTGAGTATCTT
GAPDH	Forward: AAGGTCATCCCTGAGCTGAACG
	Reverse: GGGTGTCGCTGTTGAAGTCAGA
p53	Forward: TACAAGCAGTCACAGCAGATGACGGAGGTT
	Reverse: AGTTGTAGTGGATGGTGGTACAGTCAGAG
PIG3	Forward: TGGTCACAGCTGGCTCCCAGAA
	Reverse: CCGTGGAGAAGTGAGGCAGAATTT
qPCR	
β-actin	Forward: TGAAGTGTGACGTGGACATC
	Reverse: GGAGGAGCAATGATCTTGAT
BAD	Forward: AGC CAA CCA GCA GCA GCC ATC AT
	Reverse: CTC CCC CAT CCC TTC GTC GTC
Caspase 3	Forward: GACTGCGGTATTGAGACAGA
	Reverse: CGAGTGAGGATGTGCATGAA
Caspase 7	Forward: CAACGACACCGACGCTAATC
	Reverse: GGTCCTTGCCATGCTCATTC
COX-2	Forward: TGAGCAACTATTCCAAACCAGC
	Reverse: GCACGTAGTCTTCGATCACTATC
p53	Forward: GGCGCACAGAGGAAGAGAAT
	Reverse: GGAGAGGAGCTGGTGTTGTTG
PIG3	Forward: CTCATGCCTATCCCAGAGGGATTG
	Reverse: CCACTCAGTCCTGCATGGATTAGC

RESULTS

CERAMIDE AND RESVERATROL INDUCE APOPTOSIS IN HUMAN OVARIAN CANCER OVCAR-3 CELLS

We first determined the effects of ceramide on the induction of apoptosis in human ovarian cancer OVCAR-3 cells. Cells were treated with 1–50 µM ceramide or resveratrol and harvested after 48 h exposure. To test for effects on induction of apoptosis, expression of BcL-x-s, a pro-apoptotic protein, was measured by immunoblot analysis. Agent-induced apoptosis was indicated by either changes in relative nucleosome content determined by nucleosome ELISA or DNA fragmentation assay. Results in Figure 1 show that the level of the pro-apoptotic protein, BcL-x-s, which is considered a dominant negative inhibitor of anti-apoptotic proteins, BcL-x-l and BcL-2, was significantly increased in ceramide-treated cells as was the expression of relative nucleosome content. The *bcl-x* gene encodes two distinct proteins as a result of alternative splicing, a long form (BcL-x-l, apparent MW 29–30 kDa) and a short form (BcL-x-s, apparent MW 21–26 kDa). Resveratrol-induced apoptosis shown by BcL-x-s

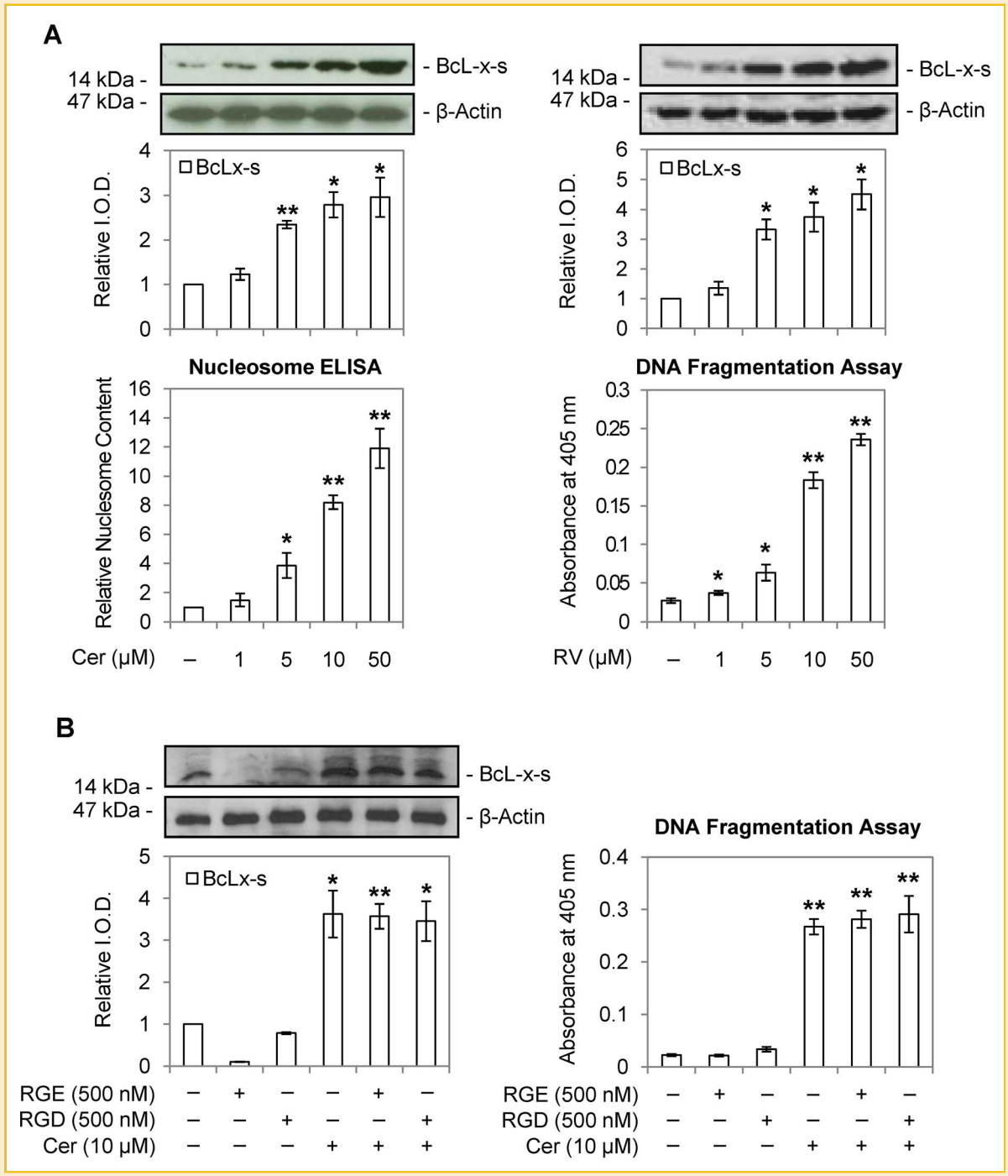

Fig. 1. Ceramide and resveratrol induce apoptosis in human ovarian cancer cells. A: OVCAR-3 cells were treated with ceramide (1–50 μM) or resveratrol (1–50 μM) for 48 h. Upper panel: Cytosolic proteins were separated by SDS–PAGE and blotted with anti-BcL-x-s antibody. β-actin was used as an internal control of cytosolic extracts. Number of independent experiments (N) = 4. Lower panel: Ceramide or resveratrol-induced apoptosis were determined by nucleosome ELISA (Ceramide) or DNA fragmentation (Resveratrol) as described in the Materials and Methods Section. N = 4. $^{**}P < 0.01$ compared with untreated control, $^{*}P < 0.05$ compared with untreated control. B: OVCAR-3 cells were treated with ceramide (10 μM) in the presence or absence of RGD (500 nM) or RGE (500 nM) peptides for 48 h. Cytosolic proteins were separated by SDS–PAGE and blotted with anti-BcL-x-s antibody. Ceramide-induced apoptosis was determined by DNA fragmentation as described in the Materials and Methods Section. N = 3. $^{**}P < 0.01$ compared with untreated control, $^{*}P < 0.05$ compared with untreated control. Cer, ceramide; RV, resveratrol; I.O.D., integrated optical density.

accumulation and DNA fragmentation assay was also concentration-dependent (Fig. 1A) as we have shown previously [Lin et al., 2011a]. Resveratrol binds to the membrane-associated receptor, integrin αvβ3 [Lin et al., 2006, 2008b, 2011a] to induce apoptosis which can be blocked by co-incubation of RGD (Arg-Gly-Asp) peptide. To test whether the effects of ceramide might involve binding to integrin αvβ3, cells were treated with ceramide for 48 h in the presence or absence of RGD peptide which has been used to block ligand binding to integrin αvβ3, and compared with cells treated with non-functional RGE (Arg-Gly-Glut) peptide [Lin et al., 2006, 2008b]. When cells were treated with ceramide for 48 h in the presence or absence of RGD peptide, the accumulation of BcL-x-s induced by ceramide was not affected by either RGD or RGE peptide suggesting that the effects of ceramide did not require binding to integrin αvβ3 (Fig. 1B, left-hand panel). Similar results were observed in apoptosis conducted by DNA fragmentation assay (Fig. 1B, right-hand panel).

ACTIVATION OF ERK1/2 AND P38 KINASE IS ESSENTIAL FOR CERAMIDE-INDUCED COX-2 ACCUMULATION AND APOPTOSIS

Previously, we have shown that resveratrol induces nuclear COX-2 accumulation and Ser-15 phoshorylation of p53 in many cancer cells [Tang et al., 2006; Lin et al., 2008a, 2011a]. It is of interest to study if ceramide also induces nuclear accumulation of COX-2 and Ser-15 phosphorylation of p53 in parallel with apoptosis in OVCAR-3 cells. OVCAR-3 cells were treated with different concentrations of ceramide or resveratrol for 48 h, the optimal time period to detect signal transduction involved in ceramide/resveratrol-induced apoptosis. Both ceramide and resveratrol induced nuclear COX-2 accumulation and Ser-15 phosphorylation of p53 in a concentration-dependent manner (Fig. 2A). In contrast, the abundance of total COX-1 was not affected by both agents (Fig. 2A). To test whether exposure to ceramide affected nuclear COX-2 gene expression, OVCAR-3 cells were treated with 10 μM ceramide for 48 h, harvested, and COX-2 expression quantified by RT-PCR. In parallel, cells treated with 10 μM resveratrol were used as a positive control. Results shown in Figure 2B indicated that both ceramide and resveratrol induced COX-2 gene expression. Real-time PCR was also conducted to show that both ceramide and resveratrol induced COX-2 expression (Fig. 2B, right lower panel).

The induction of nuclear COX-2 accumulation by resveratrol in several types of cancer cells is activated in an ERK1/2-dependent manner [Tang et al., 2006; Lin et al., 2008a,b]. In order to examine which signal transduction pathway plays a role in ceramide-induced nuclear COX-2 accumulation, cells were treated with 10 μM ceramide or 10 μM resveratrol in the presence or absence of a MEK inhibitor, PD98059, or a p38 inhibitor, SB203580, for 48 h. Nuclear proteins were subjected to western blot analysis. Both PD98059 and SB203580 inhibited ceramide-induced COX-2 nuclear accumulation (Fig. 3A). On the other hand, resveratrol-induced nuclear accumulation of COX-2 was only inhibited by MEK inhibitor, PD98059 (Fig. 3A). PD98059 and SB203580 inhibited the activation of ERK1/2 or p38 kinase which activated by ceramide or resveratrol (Fig. 3A). We also examined the signal transduction pathway involved in ceramide- or resveratrol-induced apoptosis in OVCAR-3 cells. Results presented in Figure 3B indicated that apoptosis measured by caspase-3 activity resulting from exposure to 10 μM ceramide was effectively blocked by both PD98059 (30 μM) and SB203580 (10 μM) and resveratrol-induced apoptosis only inhibited by PD98059 (Fig. 3B). These results suggest that while resveratrol-induced apoptosis is dependent on activated ERK1/2 (Fig. 3B) [Tang et al., 2006; Lin et al., 2008a,b], apoptosis elicited by ceramide occurred via ERK1/2 and p38 kinase activation signal transduction pathways. Apoptosis associated DNA fragmentation also indicated that ceramide-induced apoptosis is ERK1/2- and p38 kinase-dependent and that of resveratrol is via ERK1/2 signal transduction pathway (Fig. 3B).

INDUCIBLE COX-2 ENGAGES IN CERAMIDE- AND RESVERATROL-INDUCED APOPTOSIS IN OVARIAN CANCER CELLS

Resveratrol-induced apoptosis is inducible COX-2-dependent [Tang et al., 2006; Lin et al., 2008a,b, 2011a]. In order to study if inducible COX-2 binds to pro-apoptotic gene promoters, ovarian cells treated with ceramide or resveratrol were cross-linked and chromatin immunoprecipitation was performed using anti-COX-2 antibody to pull down the COX-2-associated DNA sequence. Results presented in Figure 4A indicated that COX-2 binds to the *PIG3* promoter in ceramide- and resveratrol-treated OVCAR-3 cells. Quantitative real-time PCR of the *PIG3* promoter also supported the observation (Fig. 4A, right panel).

To examine if inducible COX-2 is essential for ceramide-induced Ser-15 phosphorylation of p53 in OVCAR-3 cells, the specific COX-2 inhibitor (NS398) was used. When OVCAR-3 cells were treated with 10 μM ceramide or 10 μM resveratrol in the presence or absence of a specific COX-2 inhibitor, NS398 (10 μM), ceramide- or resveratrol-induced nuclear COX-2 accumulation and Ser-15 phosphorylation of p53 were inhibited by NS398 (Fig. 4B), while the effect persisted using the non-specific COX-2 inhibitor, indomethacin (10 μM) ($P = 0.66$). Interestingly, ERK1/2 activation induced by ceramide and resveratrol was not affected by either NS398 or indomethacin confirming our previous conclusion that ERK1/2 activation is upstream of COX-2 expression and Ser-15 phosphorylation of p53 [Tang et al., 2006; Lin et al., 2008a, 2011a].

To further demonstrate that inhibition of inducible COX-2 accumulation blocks ceramide-induced apoptosis in OVCAR-3 cells, COX-2-*siRNA* was used to reduce amounts of cellular COX-2. Cells transfected with *COX-2-siRNA* or non-functional *scRNA* were then treated with 10 μM ceramide or 10 μM resveratrol for 48 h. The nuclear accumulated COX-2 decreased in *siRNA* transfected cells. Similarly, the relative levels of Ser-15 phosphorylated p53 in cells which treated with ceramide or resveratrol and concurrently transfected with COX-2 *siRNA* (but not *scRNA*) dropped to values comparable to the expression observed in control cells (Fig. 5A). By contrast, the total cellular COX-1 and ceramide- or resveratrol-induced ERK1/2 activation were not affected by either *siRNA* of COX-2 or *scRNA* (Fig. 5A). Parallel experiments were conducted for anti-proliferational studies by nucleosome ELISA and results presented in Figure 5B indicated that functional COX-2 is essential for the induction of apoptosis by ceramide and resveratrol.

CERAMIDE- AND RESVERATROL-INDUCED APOPTOSIS IS ACTIVATED P53-DEPENDENT IN OVARIAN CANCER CELLS

Previously, we have shown that resveratrol induces p53 dependent apoptosis [Lin et al., 2002, 2008a,b; Shih et al., 2002]. To gain information on ceramide-mediated induction of p53 in relation to apoptosis, OVCAR-3 cells were treated with ceramide or resveratrol in the presence or absence of p53 inhibitor, PFT-α [Lin et al., 2002].

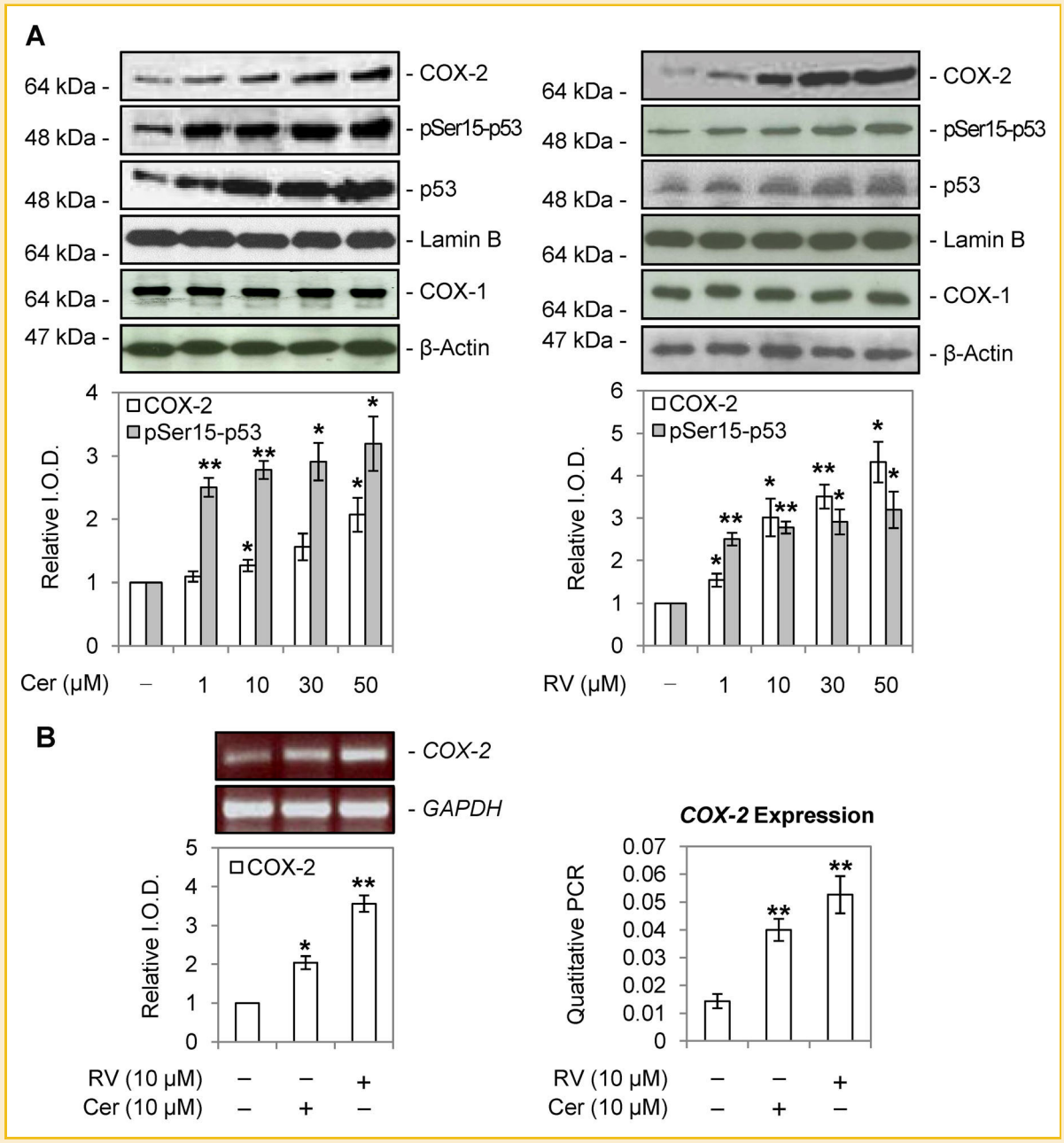

Fig. 2. Ceramide and resveratrol induce nuclear accumulation of COX-2 and Ser-15 phosphorylation of p53 in OVCAR-3 cells. A: OVCAR-3 cells were treated with ceramide (1–50 μM) or resveratrol (1–50 μM) for 48 h. Whole cell lysates were separated by SDS–PAGE and blotted with anti-COX-1 antibody. Nuclear proteins were separated by SDS–PAGE and blotted with anti-phospho-ser-15 p53 and COX-2 antibodies. β-actin or lamin-B was used as an internal control of whole lysate or nuclear extracts. N = 3. B: OVCAR-3 cells were treated with 10 μM ceramide or 10 μM resveratrol for 48 h. Cells were harvested and total RNA was extracted and RT-PCR or quantitated PCR was performed as described in the Materials and Methods Section. N = 3. $^{*}P < 0.05$ compared with untreated control, $^{**}P < 0.01$ compared with untreated control. Cer, ceramide; RV, resveratrol; I.O.D., integrated optical density.

Results shown in Figure 6A indicated that PFT-α inhibited both ceramide- and resveratrol-induced serine 15 phosphorylation of p53. Studies also indicated that several p53-dependent pro-apoptotic genes such as *p53*, and *PIG3* increased in expression when cells were treated with ceramide or resveratrol (Fig. 6B). Ceramide- and resveratrol-induced apoptosis was inhibited by PFT-α as well (Fig. 6C). These results suggest that ceramide-induced apoptosis is inducible COX-2- and p53-dependent in human ovarian cancer cells as also observed for resveratrol [Lin et al., 2011a].

CERAMIDE AND RESVERATROL SHARE A SIMILAR MECHANISM TO INDUCE APOPTOSIS

Resveratrol reportedly activates a ceramide-dependent signal transduction pathway [Scarlatti et al., 2003] and our previous studies

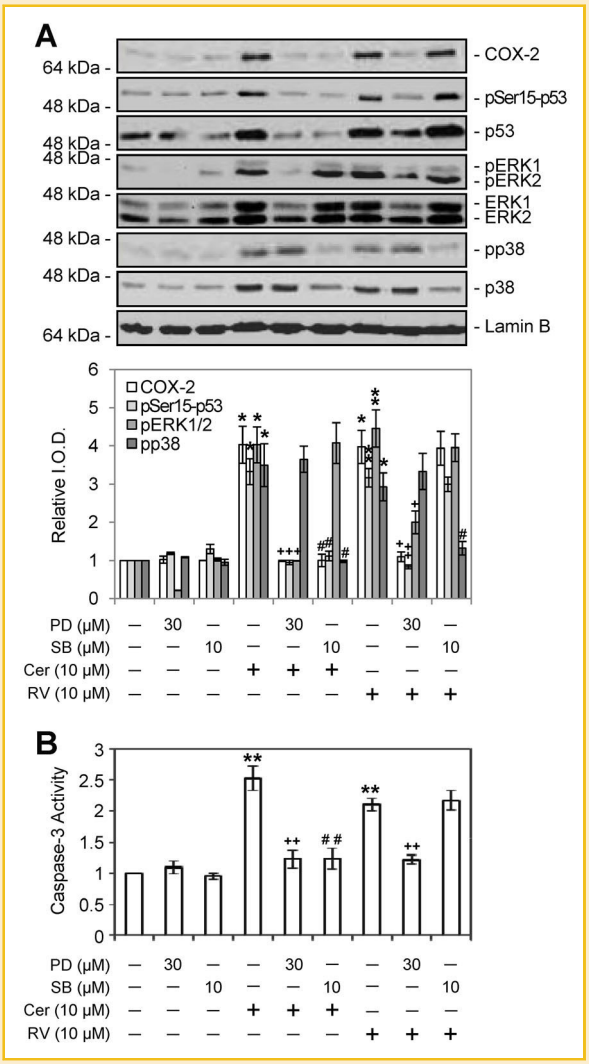

Fig. 3. Ceramide and resveratrol share activated ERK1/2-dependent signal transduction pathways to induce apoptosis in OVCAR-3 cells. A: OVCAR-3 cells were treated with 10 μM ceramide or 10 μM resveratrol in the presence or absence of 30 μM PD98059 or 10 μM SB 203580 for 48 h. Nuclear proteins were separated by SDS–PAGE and blotted with anti-phospho-Ser-15 p53, COX-2, pp38 and pERK1/2 antibodies. Lamin B was used as an internal control of nuclear extracts. N = 4. $^{**}P < 0.01$ compared with untreated control. $^{*}P < 0.05$ compared with untreated control. $^{+}P < 0.05$ compared between with/without PD98059 treatment. $^{\#}P < 0.05$ compared between with/without SB203580 treatment. B: OVCAR-3 cells were treated with 10 μM ceramide or 10 μM resveratrol in the presence or absence of 30 μM PD98059 or 10 μM SB203580 for 48 h. Apoptosis induced by ceramide and resveratrol was determined by caspase-3 activity. N = 3. $^{**}P < 0.01$ compared with untreated control. $^{++}P < 0.01$ compared between with/without PD98059 treatment. $^{\#\#}P < 0.01$ compared between with/without SB203580 treatment.

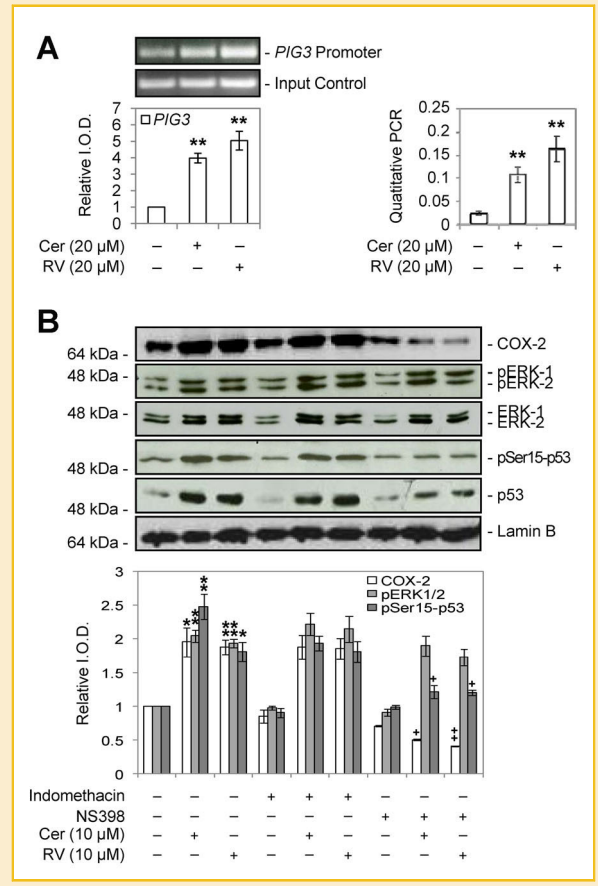

Fig. 4. Nuclear COX-2 complexes with *PIG3* promoter in ceramide- or resveratrol-treated OVCAR-3 cells. A: OVCAR-3 cells were treated with 20 μM ceramide or resveratrol for 48 h and cells were fixed for ChIP as described in the Materials and Methods Section. ChIP was performed using anti-COX-2 antibody and sequence of *PIG3* promoter. Shown at the lower panel is a graph of *PIG3* promoter image intensity of qPCR relative to the input control. N = 4. $^{**}P < 0.01$ compared with untreated control. B: OVCAR-3 cells were treated with 10 μM ceramide or 10 μM resveratrol for 48 h in the presence or absence of a specific COX-2 inhibitor, NS398 (10 μM), or non-specific COX-2 inhibitor, indomethacin (10 μM). Nuclear proteins were separated by SDS–PAGE and blotted with anti-phospho-Ser-15 p53, COX-2, and pERK1/2 antibodies. Lamin B was used as an internal control of nuclear extracts. N = 4. $^{**}P < 0.01$ compared to untreated control; $^{*}P < 0.05$ compared to untreated control; $^{++}P < 0.01$ compared between without/with NS398-treated resveratrol-treated samples; $^{+}P < 0.05$ compared between without/with NS398-treated ceramide- or resveratrol-treated samples. Cer, ceramide; RV, resveratrol; I.O.D., integrated optical density.

have shown that resveratrol induces apoptosis in cancer cells by binding to a membrane-associated receptor, integrin αvβ3 [Lin et al., 2006, 2008b, 2011a]. Since integrins are known to play a role in endocytosis [Dupuy and Caron, 2008; Caswell et al., 2009] and are indirectly linked to the cytoskeleton, we investigated whether F-actin reorganization is involved in the pro-apoptotic action of ceramide and resveratrol. Cells were treated with either resveratrol or ceramide, with or without addition of the endocytosis inhibitor, cytochalasin D (CytD) which also inhibits F-actin reorganization [Sexton et al., 2004; Holzer and Howell, 2006]. Both resveratrol and ceramide induced pro-apoptotic protein BcL-x-s; however, the expression of BcL-x-s was reduced substantially in cells co-exposed to CytD for 48 h. Here, cells treated with resveratrol showed more significant concentration-dependent reduction in response to co-treatment by CytD compared to a decrease in BcL-x-s by CytD in ceramide treated cells (Fig. 7A, upper panel). Correspondingly, ceramide- and resveratrol-induced apoptosis measured by nucleosome ELISA was also inhibited by CytD (Fig. 7A, lower panel).

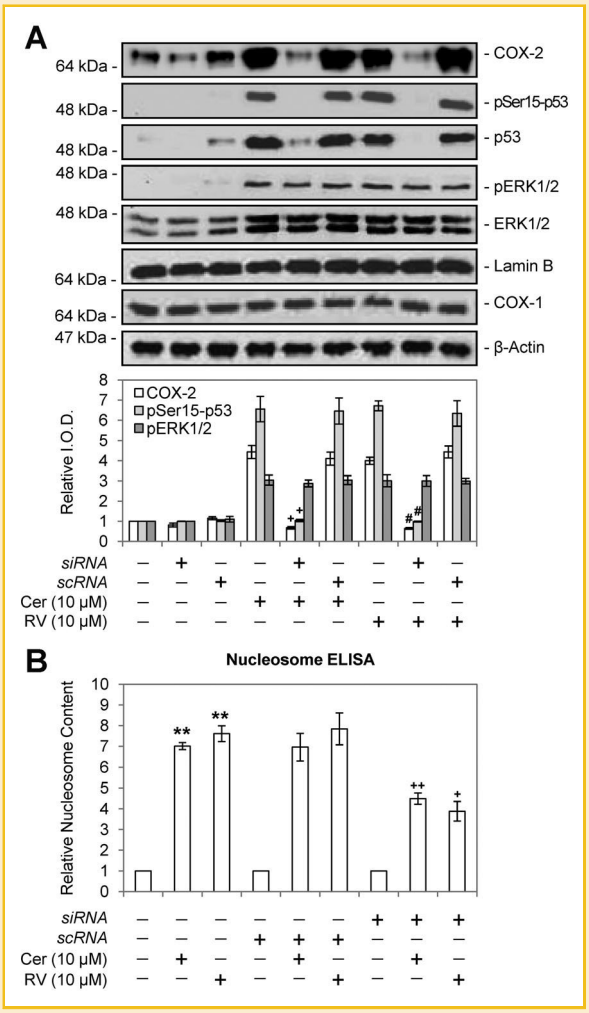

Fig. 5. Inducible COX-2 is essential for ceramide- and resveratrol-induced apoptosis in OVCAR-3 cells. A: OVCAR-3 cells were pre-exposed to COX-2 *siRNA* or *scRNA* for 24 h and then treated with 10 μM ceramide or 10 μM resveratrol for 48 h. Nuclear proteins were separated by SDS–PAGE and blotted with anti-phospho-Ser-15 p53 COX-2, pp38 and pERK1/2 antibodies. Cytosolic proteins were separated by SDS–PAGE and blotted with anti-COX-1 antibody. Lamin B was used as an internal control of nuclear extracts while β-actin was used as an internal control for cytosolic extracts. N = 4. $^{+,\#}P < 0.01$ compared between without/with COX-2 *siRNA*-presented ceramide- or resveratrol-treated samples. B: OVCAR-3 cells were pre-treated with COX-2 *siRNA* or *scRNA* for 24 h and then were treated with 10 μM ceramide or 10 μM resveratrol for 48 h and apoptosis examined by nucleosome ELISA. N = 4. $^{**}P < 0.01$ compared to untreated control; $^{++}P < 0.01$ compared between without/with *siRNA*-presented ceramide-treated samples; $^{+}P < 0.05$ compared between without/with *siRNA*-presented resveratrol-treated samples. Cer, ceramide; RV, resveratrol.

To differentiate further between mechanisms involved in resveratrol and ceramide-induced apoptosis in ovarian cancer cells, OVCAR-3 cells were treated with 10–100 μM of resveratrol or ceramide. Since a loss of trans-membrane potential in mitochondria is one of a few key events that occur during mitochondria-mediated apoptosis, mitochondrial trans-membrane potential was assayed by flow cytometry using a mitochondrial membrane potential assay kit. Results indicate that ceramide-treated cells underwent a dose-dependent reduction in trans-membrane potential when compared to untreated cells (Fig. 7B). However, the loss of potential in resveratrol-treated OVCAR-3 cells was not significant (Fig. 7B). These results suggest that ceramide, but not resveratrol, induces apoptosis by a mitochondria-dependent mechanism.

Caspase-3 and caspase-7 are activated in the apoptotic cells by both extrinsic (death ligand) and intrinsic (mitochondrial) pathways [Roy and Nicholson, 2000]. Ceramide induced expression of both caspase-3 and caspase-7 in OVCAR-3 cells. This expression was inhibited by NS398 (Fig. 7C). On the other hand, resveratrol, while similarly inducing the expression of caspase-3 and 7, only showed abrogation of caspase-3 induction by treatment with NS398 (Fig. 7C, upper panel). Real-time PCR was also conducted and the results supported the observation (Fig. 7C, lower panel). Shown by caspase-3 activity assay, ceramide- and resveratrol-induced apoptosis was also inhibited by NS398 (Fig. 7D).

COMBINATION EFFECT OF CERAMIDE AND RESVERATROL

Results indicated that ceramide and resveratrol partially share signal transduction pathways to induce apoptosis in human ovarian cancer OVCAR-3 cells. Thus, it was of interest to investigate if the apoptotic effect of the two agents interacts with each other. Cell cultures were treated with ceramide (1 or 10 μM), resveratrol (1 or 10 μM), or combination for 48 h. The ceramide-induced COX-2 accumulation and Ser-15 phosphorylation of p53 was enhanced by the presence of resveratrol (Fig. 8A). Additionally, the ceramide-induced apoptosis measured by caspase-3 activity was enhanced by the presence of resveratrol significantly (Fig. 8B). Our results clearly showed that the combined treatment of ceramide and resveratrol at 1 μM induced not only more nuclear COX-2 accumulation and Ser-15 phosphorylated p53 but also more apoptosis than that of a signal agent. Although the combined treatment with 10 μM ceramide and resveratrol did not increase COX-2 and Ser-15 phosphorylated p53 significantly, the combination of ceramide and resveratrol-induced apoptosis was significantly increased as compared to either ceramide or resveratrol alone.

DISCUSSION

Results in this study indicated that ceramide and resveratrol utilize an endocytic- and activated ERK1/2-dependent pathway to induce apoptosis in human ovarian cancer OVCAR-3 cells. Exposure to ceramide and resveratrol induced expression and nuclear accumulation of COX-2 without change in total cellular COX-1. Both agents induced Ser-15 phosphorylation of p53, as well as BcL-x-s accumulation in a concentration-dependent manner that is blocked by PD98059, a MEK inhibitor. Additionally, ceramide-induced nuclear accumulation of COX-2 and BcL-x-s accumulation was blocked by a p38 inhibitor, SB 203580. It is notable to mention that nuclear accumulation of COX-2 was also blocked in ceramide-treated cells when a p38 kinase inhibitor was added, showing that while ceramide and resveratrol share an ERK1/2-dependent pathway, ceramide also utilizes a p38 kinase-dependent pathway. We have previously shown that inducible nuclear COX-2 plays a role in the activation of p53-mediated apoptosis in the presence of resveratrol [Tang et al., 2006; Lin et al., 2008a,b, 2011a]. These results revealed

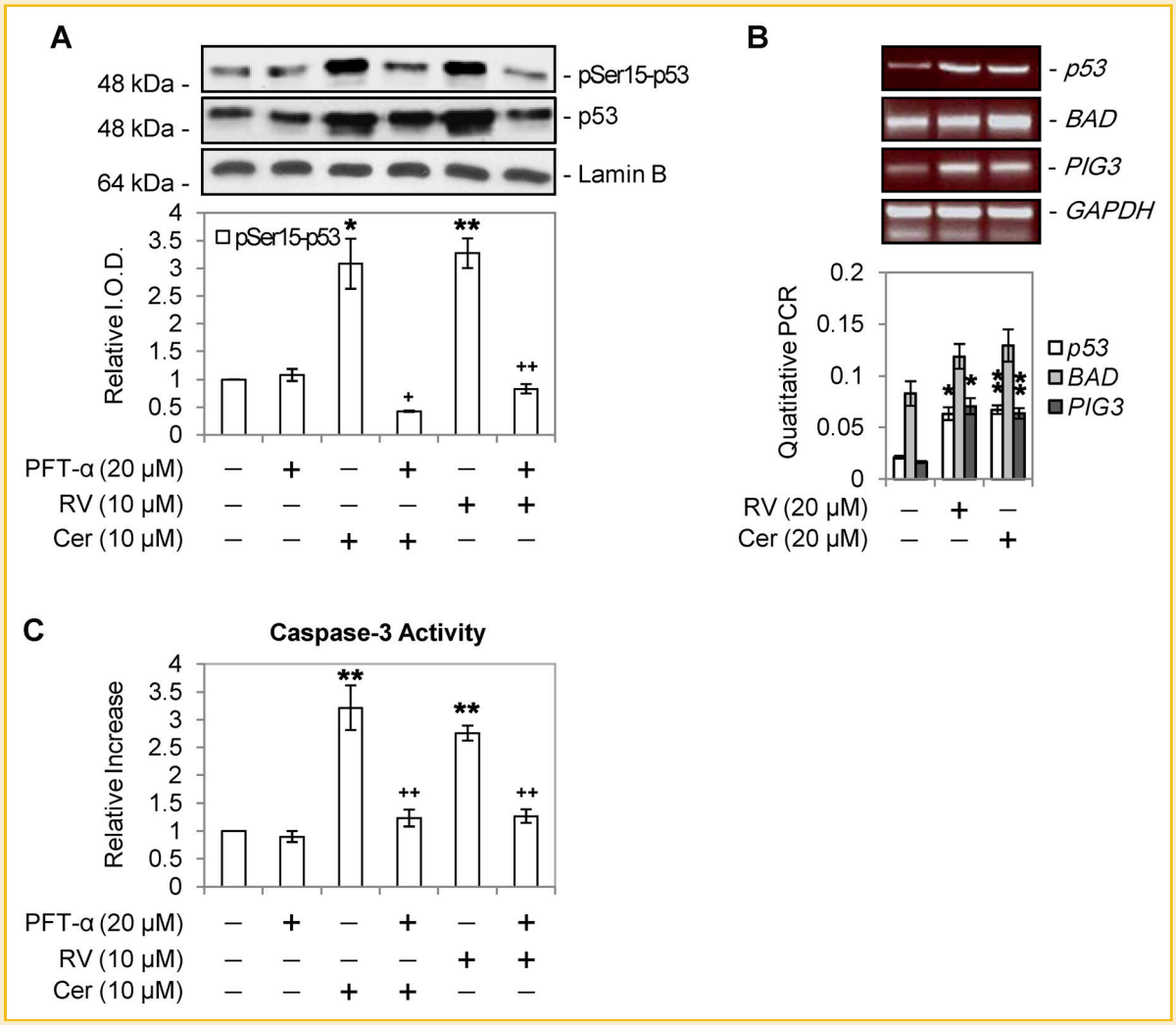

Fig. 6. Ceramide- and resveratrol-induced apoptosis is activated p53-dependent in OVCAR-3 cells. A: OVCAR-3 cells were treated with 10 μM ceramide or 10 μM resveratrol in the presence or absence of PFT-α (20 μM), a specific p53 inhibitor, for 48 h. Cells were harvested and processed as described in the Materials and Methods Section. Nuclear extracts were separated on SDS–PAGE and blotted with anti-phosopho-Ser-15 p53 antibody. Lamin B was used as an internal control. N = 4. $^{*}P < 0.05$ compared between ceramide and untreated control; $^{**}P < 0.01$ compared between resveratrol and untreated control; $^{+}P < 0.05$ compared between without/with PFT-α-treated in ceramide-treated samples; and $^{++}P < 0.01$ compared between without/with PFT-α-treated in resveratrol-treated samples. B: OVCAR-3 cells were treated with 20 μM ceramide or 20 μM resveratrol for 48 h. Cells were harvested and total RNA was extracted and RT-PCR or quantitated PCR of p53-responsive genes was performed as described in the Materials and Methods Section. N = 3. $^{**}P < 0.01$: compared with untreated control, $^{*}P < 0.05$ compared with untreated control. C: OVCAR-3 cells were treated with 10 μM ceramide or 10 μM resveratrol in the presence or absence of PFT-α (20 μM) and apoptosis examined by caspase-3 activity assay. N = 3. $^{**}P < 0.01$ compared to untreated control, $^{++}P < 0.01$ compared between without/with PFT-α-presented ceramide- or resveratrol-treated samples. Cer, ceramide; RV, resveratrol.

that ceramide operates by signaling pathway and mechanisms that partially overlaps with those elicited by resveratrol, primarily in invoking endocytosis, activation of ERK1/2, accumulation of nuclear COX-2 and p53 activation and expression of caspases-3 and -7, to induce apoptosis.

COX-2, the rate-limiting enzyme in prostaglandin synthesis, is induced in many cells by inflammatory mediators [Xu et al., 1999]. Expression of *COX-2* in cell and animal models is associated with tumor cell growth and metastasis, enhanced cellular adhesion and inhibition of apoptosis [Van der Donk et al., 2002; Dixon, 2004]. The mechanisms of these tumor-promoting actions of COX-2 are incompletely understood. Pharmacologic inhibitors of COX-2 can decrease tumor cell growth or prevent tumorigenesis in animal models of cancer [Evans, 2003; Rüegg et al., 2003; Yao et al., 2004] and may decrease growth of certain human tumors [King and Khalili, 2001; Mishra et al., 2004]. However, the nature of the relationship of COX-2 protein to cancer cell growth is more complex than the foregoing evidence infers and this is suggested by reports that COX-2 may be pro-apoptotic [Trifan et al., 1999; Zahner et al., 2002] and that pharmacologic induction of COX-2 expression results in inhibition of colon cancer cell growth [Williams et al., 2003]. Treatment of human glioblastoma and medulloblastoma cells with the non-steroidal anti-inflammatory drug flurbiprofen has been shown to enhance COX-2 expression, to cause complex

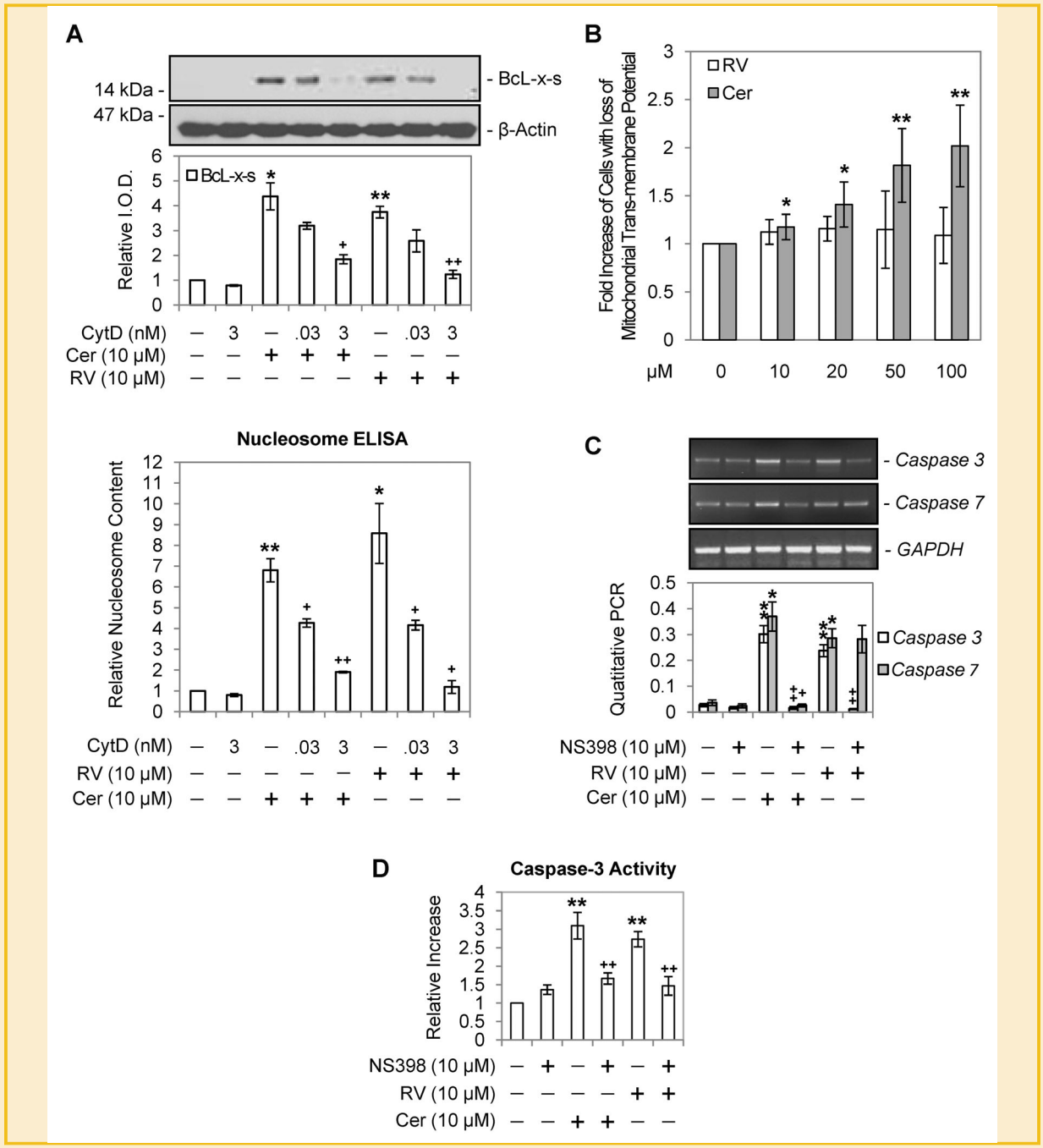

Fig. 7. Requirements for endocytosis in resveratrol- and ceramide-induced apoptosis in OVCAR-3 cells and change of mitochondrial potential. A: Upper panel: OVCAR-3 cells were treated with resveratrol (10 μM) or ceramide (10 μM) in the presence or absence of CytD (0.03 and 3 μM) for 48 h. Cytosolic proteins were extracted, separated by SDS–PAGE and western blots were conducted by using ant-BcL-x-s antibody. N = 3. Lower panel: OVCAR-3 cells were treated with resveratrol (10 μM) or ceramide (10 μM) in the presence or absence of CytD (0.03 and 3 nM) for 48 h. Resveratrol and ceramide induced apoptosis determined by nucleosome ELISA as described in the Materials and Methods Section. N = 3. $^{**}P < 0.01$ compared to untreated control; $^{*}P < 0.05$ compared to untreated control; $^{++}P < 0.01$ compared between without/with CytD presented resveratrol-treated samples; $^{+}P < 0.05$ compared between without/with CytD presented ceramide-treated samples. Lower panel: $^{**}P < 0.01$ compared to untreated control; $^{*}P < 0.05$ compared to untreated control; $^{++}P < 0.01$ compared between without/with CytD presented ceramide-treated samples; $^{+}P < 0.05$ compared between without/with CytD presented ceramide- or resveratrol-treated samples. B: OVCAR-3 cells were treated with 10, 20, 50, or 100 μM ceramide or resveratrol for 24 h. Cells were then harvested, washed and centrifuged to pellet approximately 1×10^6 cells. JC-1 Staining Solution was added to each sample before incubating for 30 min at 37°C. Samples were then analyzed using flow cytometry. N = 4. $^{**}P < 0.01$ compared with untreated control; $^{*}P < 0.05$ compared with untreated control. C: OVCAR-3 cells were treated with 10 μM ceramide or 10 μM resveratrol in the presence or absence of NS398 (10 μM). Cells were harvested and total RNA was extracted and RT-PCR and quantitated PCR of caspase-3 and caspase-7 were conducted as described. N = 3. $^{**}P < 0.01$ compared to untreated control; $^{*}P < 0.05$ compared to untreated control; $^{++}P < 0.01$ compared between without/with NS398-treated ceramide-/resveratrol-treated samples; and $^{+}P < 0.05$ compared between without/with NS398-treated ceramide-treated samples. D: OVCAR-3 cells were treated with 10 μM ceramide or 10 μM resveratrol in the presence or absence of NS398 (10 μM) and apoptosis examined by caspase-3 activity assay. N = 3. $^{**}P < 0.01$ compared to untreated control; $^{++}P < 0.01$ compared between without/with NS398-presented ceramide- or resveratrol-treated samples. Cer, ceramide; RV, resveratrol.

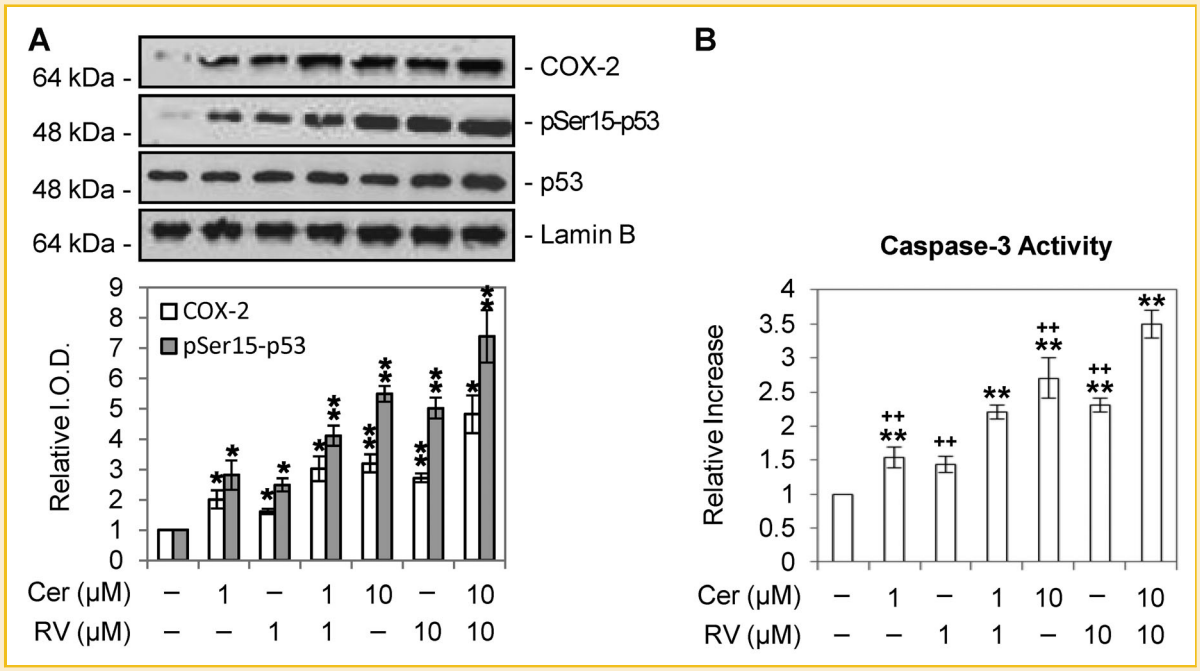

Fig. 8. Effect of combination treatment of ceramide and resveratrol on OVCAR-3 cells. A: Cells were treated with ceramide (1 or 10 μM), resveratrol (1 or 10 μM) or combination for 48 h. Nuclear proteins were separated by SDS–PAGE and blotted with anti-COX-2 or anti-Ser-15 phosphorylated p53 antibody, respectively. Lamin-B was used as an internal control. N = 3. $^{**}P < 0.01$ compared with untreated control; $^{*}P < 0.05$ compared with untreated control. B: Cells were treated with ceramide (1 or 10 μM), resveratrol (1 or 10 μM) or combination for 48 h. Ceramide or resveratrol-induced apoptosis was determined by caspase-3 activity assay as described in the Materials and Methods Section. N = 4. $^{**}P < 0.01$ compared with untreated control; $^{*}P < 0.05$ compared with untreated control. $^{++}P < 0.01$ compared between combination and single agent. Cer, ceramide; RV, resveratrol.

formation of COX-2 protein with p53 and to suppress tumor growth [King and Khalili, 2001]. Overexpression of COX-2 inhibits platelet-derived growth factor-induced proliferation via the induction of p53, as well as that of p21 [Zahner et al., 2002]. Furthermore, research by Parfenova et al. [2001] indicate that COX-2 is mainly a nuclear resident possibly connected with the nuclear matrix in quiescent cells of endothelial cells from porcine and human cerebral microvessels and from human umbilical vein. Studies by Parfenova et al. [2001] indicate that nuclear COX-2 in vascular endothelial cells is associated with the nuclear matrix that spatially organizes chromatin; the association implies the involvement of COX-2 in essential nuclear activities such as transcription, replication, and regulation of gene expression [Nickerson et al., 1995; Pederson, 1998; Hancock, 2004]. Patel et al. [1999] have shown that stimulation of murine RAW 264.7 macrophages with lipopolysaccharide (LPS) causes 90% of COX-2 to localize in the nuclear fraction and ~10% in cytoplasm. In quiescent endothelial cells from human umbilical vein, porcine, and human cerebral microvessels, COX-2 is also found principally in the nucleus [Parfenova et al., 1997, 2001]. In endothelial cells, COX-2 has been found to traffic between the nucleus and the cytoplasm and localize at sites of active transcriptional sites in nucleus which indicates a novel function of COX-2 in regulating gene expression [Parfenova et al., 2001]. Our results also indicated that nuclear accumulated COX-2 bound with *PIG3* promoter in ceramide- and resveratrol-treated OVCAR-3 cells (Fig. 4A) and resveratrol-treated human breast cancer [Tang et al., 2006] and head and neck carcinoma cells [Lin et al., 2008b].

The COX-2 specific inhibitor, NS398, but not the non-specific inhibitor, indomethacin inhibited Ser-15 phosphorylation of p53 induced by ceramide and resveratrol (Fig. 4B) suggesting that inducible COX-2 is involved in p53 phosphorylation and downstream p53-dependent apoptosis (Fig. 5B). Although both indomethacin and NS398 have been reported to induce apoptosis, ceramide- and resveratol-induced COX-2 expression was affected by NS389 but not indomethacin. Therefore, without nuclear COX-2 accumulation, p53 phosphorylation and p53-dependent apoptosis were inhibited. In addition, indomethacin-induced apoptosis in esophageal adenocarcinoma cells is independent of COX-2 expression [Aggarwal et al., 2000].

Ceramide induces apoptosis [Zhao et al., 2004] and cell cycle arrest [Jayadev et al., 1995]. Treatment of human mammary epithelial cells with C_2-ceramide increases levels of COX-2 protein and mRNA and enhances prostaglandin E_2 synthesis [Subbaramaiah et al., 1998]. Ramer et al. [2003] have shown that R(+)-methanandamide induces COX-2 expression in human neuroglioma cells via production of ceramide. Recently, studies have shown that resveratrol induces apoptosis through a ceramide signal transduction pathway [Scarlatti et al., 2003; Dimanche-Boitrel et al., 2005]. It is therefore reasonable to speculate that the induction by resveratrol of COX-2-dependent apoptosis may share signal transduction pathways with ceramide.

Endocytosis plays an important role for the entry of ligands into cells. Both ceramide (Fig. 7) and resveratrol [Lin et al., 2011a] induced an increase in BcL-x-s, a pro-apoptotic protein, in OVCAR-3 cells. CytD inhibits endocytosis and F-actin reorganization, and caused a

reduction in the amount of BcL-x-s and apoptosis in OVCAR-3 cells treated with resveratrol. Similar results were noted in cells treated with ceramide and CytD; however, BcL-x-s and apoptosis were reduced to a lesser degree in ceramide-treated cells than in resveratrol-treated cells. Similarly, ceramide-induced apoptosis was not affected by RGD peptide, which is known to interfere with resveratrol binding to integrin αvβ3 [Lin et al., 2006, 2008b]. These findings, coupled with the recent demonstration that endocytosis elicited by resveratrol occurred via binding to integrin αvβ3 [Lin et al., 2006, 2008b, 2011b; Hsieh et al., 2011] and lipid rafts [Colin et al., 2011] to activate signal transduction, suggest that divergent mechanisms are operative in the induction of apoptosis by ceramide and resveratrol.

An important observation revealed in this study relates to the nuclear accumulation of COX-2 in the context of p53 phosphorylation changes and induction of apoptosis induced by ceramide. Blocking COX-2 accumulation by either an inhibitor specific to COX-2, NS398, or *siRNA* resulted in a reduced amount of Ser-15 phosphorylation of p53 as well as a significant attenuation of apoptosis, despite activation of ERK1/2 being sustained [Tang et al., 2006]. Kim et al. showed that phytosphingosine derivatives, *N*-acetyl phytosphingosine (NAPS) and tetra-acetyl phytosphingosine (TAPS), elevate *COX-2* expression via tyrosine kinase and PKC, with subsequent ERK activation. p38 is not involved in NAPS-mediated *COX-2* expression, but does play a role in TAPS-mediated expression [Kim et al., 2003]. Other reports indicate that induction of COX-2 by ceramide is ERK- and p38-dependent [Subbaramaiah et al., 2000; Ramer et al., 2003]. That COX-2 potentially plays a role in regulating the transcription of p53-responsible genes in ceramide-treated cells is supported by an increase in COX-2 binding to the *PIG3* promoter when compared to untreated cells, suggesting that nuclear accumulation of COX-2 is critical to the functioning of ceramide in apoptosis. We also observed that ceramide, as well as resveratrol, induced the expression of caspase-3 and caspase-7 in OVCAR-3 cells (Fig. 7C). Pharmacologic inhibition of COX-2 activity in colon cancer cells has been shown to increase the nuclear localization of active p53 [Swamy et al., 2003].

p53 has been shown to play a role in mitochondria-mediated apoptosis [Chipuk et al., 2004], which is initiated by a few key events including the loss of trans-membrane potential, the release of cytochrome *c*, and changes in electron transport. Trans-membrane potential is an electrical and chemical gradient generated by unequal protons and ions on both sides of the membrane. The maintenance of this potential helps to ensure that the mitochondria functions properly. Evaluating the status of mitochondrial function is often used as one of the earliest indicators of cell death, as a collapse of potential is a sign that a cell is entering an apoptotic pathway. Given that both resveratrol and ceramide induce p53 expression, it seemed likely that ceramide would cause a loss in mitochondrial membrane potential as this is observed in HT29 human colon carcinoma cells [Martin et al., 2005] and leukemia cells [Amarante-Mendes et al., 1998]. The results suggest that ceramide does in fact involve the mitochondria to induce apoptosis in OVCAR-3 cells, while resveratrol appears to relay its signaling without utilizing the mitochondria.

In summary, this study established an inducible nuclear accumulation of COX-2-dependent mechanism of apoptosis induced by ceramide in human ovarian cancer OVCAR-3 cells which may not be applied in other ovarian cancer cells due to the different characteristics between OVCAR-3 and other ovarian cancer cells. Interestingly, the signal transduction pathways involved in ceramide-induced COX-2-dependent apoptosis partially overlapped with those elicited by resveratrol in ovarian cancer OVCAR-3 cells and other cancer cells examined [Tang et al., 2006; Lin et al., 2008a,b, 2011a]. The similarities and differences might be exploited in the use of these two agents in sequence or in combination for chemoprevention and cancer treatment.

ACKNOWLEDGMENTS

This work was supported in part by an endowment established by M. Frank and Margaret Domiter Rudy and by the start-up fund of Taipei Medical University. The authors deeply appreciate the excellent technical support of Ms. Ran Meng and the help of Mr. Russ Toombs, Ms. Susie Leavitt and Ms. Kelly Backer at Center for Medical Science, Albany, New York.

REFERENCES

Aggarwal S, Taneja N, Lin L, Orringer MB, Rehemtulla A, Beer DG. 2000. Indomethacin-induced apoptosis in esophageal adenocarcinoma cells involves upregulation of Bax and translocation of mitochondrial cytochrome C independent of COX-2 expression. Neoplasia 2:346–356.

Anantharam V, Kitazawa M, Wagner J, Kaul S, Kanthasamy AG. 2002. Caspase-3-dependent proteolytic cleavage of protein kinase Cdelta is essential for oxidative stress-mediated dopaminergic cell death after exposure to methylcyclopentadienyl manganese tricarbonyl. J Neurosci 22:1738–1751.

Amarante-Mendes GP, Naekyung Kim C, Liu L, Huang Y, Perkins CL, Green DR, Bhalla K. 1998. Bcr-Abl exerts its antiapoptotic effect against diverse apoptotic stimuli through blockage of mitochondrial release of cytochrome C and activation of caspase-3. Blood 91:1700–1705.

Bhoola S, Hoskins WJ. 2006. Diagnosis and management of epithelial ovarian cancer. Obstet Gynecol 107:1399–1410.

Caswell PT, Vadrevu S, Norman JC. 2009. Integrins: Masters and slaves of endocytic transport. Nat Rev Mol Cell Biol 10:843–853.

Chipuk JE, Kuwana T, Bouchier-Hayes L, Droin NM, Newmeyer DD, Schuler M, Green DR. 2004. Direct activation of Bax by p53 mediates mitochondrial membrane permeabilization and apoptosis. Science 303:1010–1014.

Cianchi F, Cortesini C, Magnelli L, Fanti E, Papucci L, Schiavone N, Messerini L, Vannacci A, Capaccioli S, Perna F, Lulli M, Fabbroni V, Perigli G, Bechi P, Masini E. 2006. Inhibition of 5-lipoxygenase by MK886 augments the antitumor activity of celecoxib in human colon cancer cells. Mol Cancer Ther 5:2716–2726.

Colin D, Limagne E, Jeanningros S, Jacquel A, Lizard G, Athias A, Gambert P, Hichami A, Latruffe N, Solary E, Delmas D. 2011. Endocytosis of resveratrol via lipid rafts and activation of downstream signaling pathways in cancer cells. Cancer Prev Res 4:1095–1106.

Corcoran CA, He Q, Huang Y, Sheikh MS. 2005. Cyclooxygenase-2 interacts with p53 and interferes with p53-dependent transcription and apoptosis. Oncogene 24:1634–1640.

Das DK, Sato M, Ray PS, Maulik G, Engelman RM, Bertelli AA, Bertelli A. 1999. Cardioprotection of red wine: Role of polyphenolic antioxidants. Drugs Exp Clin Res 25:115–120.

Davis PJ, Shih A, Lin HY, Martino LJ, Davis FB. 2000. Thyroxine promotes association of mitogen-activated protein kinase and nuclear thyroid hormone receptor (TR) and causes serine phosphorylation of TR. J Biol Chem 275:38032–38039.

Davis FB, Tang HY, Shih A, Keating T, Lansing L, Hercbergs A, Fenstermaker RA, Mousa A, Mousa SA, Davis PJ, Lin HY. 2006. Acting via a cell surface receptor, thyroid hormone is a growth factor for glioma cells. Cancer Res 66:7270–7275.

Dimanche-Boitrel MT, Meurette O, Rebillard A, Lacour S. 2005. Role of early plasma membrane events in chemotherapy-induced cell death. Drug Resist Update 8:5–14.

Dixon DA. 2004. Dysregulated post-transcriptional control of COX-2 gene expression in cancer. Curr Pharm Des 10:635–646.

Dupuy AG, Caron E. 2008. Integrin-dependent phagocytosis: Spreading from microadhesion to new concepts. J Cell Sci 121:1773–1783.

Evans JF. 2003. Rofecoxib (Vioxx), a specific cyclooxygenase-2 inhibitor, is chemopreventive in a mouse model of colon cancer. Am J Clin Oncol 26:S62–S65.

Hancock R. 2004. Internal organisation of the nucleus: Assembly of compartments by macromolecular crowding and the nuclear matrix model. Biol Cell 96:595–601.

Hannun YA, Linardic CM. 1993. Sphingolipid breakdown products: Anti-proliferative and tumor-suppressor lipids. Biochim Biophys Acta 1154:223–236.

Hannun YA, Obeid LM. 2011. Many ceramides. J Biol Chem 286:27855–27862.

Holzer AK, Howell SB. 2006. The internalization and degradation of human copper transporter 1 following cisplatin exposure. Cancer Res 66:10944–10952.

Hsieh TC, Wong C, Bennett DJ, Wu JM. 2011. Regulation of p53 and cell proliferation by resveratrol and its derivatives in breast cancer cells: An in silico and biochemical approach targeting integrin alphavbeta3. Int J Cancer 129:2732–2743.

Jayadev S, Liu B, Bielawska AE, Lee JY, Nazaire F, Pushkareva MYu, Obeid LM, Hannun YA. 1995. Role for ceramide in cell cycle arrest. J Biol Chem 270:2047–2052.

Kim HJ, Shin W, Park CS, Kim HO, Kim TY. 2003. Differential regulation of cyclooxygenase-2 expression by phytosphingosine derivatives, NAPS and TAPS, and its role in the NAPS or TAPS-mediated apoptosis. J Invest Dermatol 121:1126–1134.

King JG Jr, Khalili K. 2001. Inhibition of human brain tumor cell growth by the anti-inflammatory drug, flurbiprofen. Oncogene 20:6864–6870.

Lin HY, Davis FB, Gordinier JK, Martino LJ, Davis PJ. 1999a. Thyroid hormone induces activation of mitogen-activated protein kinase in cultured cells. Am J Physiol 276:C1014–C1024.

Lin HY, Shih A, Davis FB, Davis PJ. 1999b. Thyroid hormone promotes the phosphorylation of STAT3 and potentiates the action of epidermal growth factor in cultured cells. Biochem J 338:427–432.

Lin HY, Shih A, Davis FB, Tang HY, Martino LJ, Bennett JA, Davis PJ. 2002. Resveratrol induced serine phosphorylation of p53 causes apoptosis in a mutant p53 prostate cancer cell line. J Urol 168:748–755.

Lin HY, Hopkins R, Cao HJ, Tang HY, Alexander C, Davis FB, Davis PJ. 2005. Acetylation of nuclear hormone receptor superfamily members: Thyroid hormone causes acetylation of its own receptor by a mitogen-activated protein kinase-dependent mechanism. Steroids 70:444–449.

Lin HY, Lansing L, Merillon JM, Davis FB, Tang HY, Shih A, Vitrac X, Krisa S, Keating T, Cao HJ, Bergh J, Quackenbush S, Davis PJ. 2006. Integrin alphaVbeta3 contains a receptor site for resveratrol. FASEB J 20:1742–1744.

Lin HY, Tang HY, Keating T, Wu YH, Shih A, Hammond D, Sun M, Hercbergs A, Davis FB, Davis PJ. 2008a. Resveratrol is pro-apoptotic and thyroid hormone is anti-apoptotic in glioma cells: Both actions are integrin and ERK mediated. Carcinogenesis 29:62–69.

Lin HY, Sun M, Tang HY, Simone TM, Wu YH, Grandis JR, Cao HJ, Davis PJ, Davis FB. 2008b. Resveratrol causes COX-2- and p53-dependent apoptosis in head and neck squamous cell cancer cells. J Cell Biochem 104:2131–2142.

Lin HY, Sun M, Tang HY, Lin C, Luidens MK, Mousa SA, Incerpi S, Drusano GL, Davis FB, Davis PJ. 2009. L-Thyroxine vs. 3,5,3'-triiodo-L-thyronine and cell proliferation: Activation of mitogen-activated protein kinase and phosphatidylinositol 3-kinase. Am J Physiol Cell Physiol 296:C980–C991.

Lin C, Crawford DR, Lin S, Hwang J, Sebuyira A, Meng R, Westfall JE, Tang HY, Lin S, Yu PY, Davis PJ, Lin HY. 2011a. Inducible COX-2-dependent apoptosis in human ovarian cancer cells. Carcinogenesis 32:19–26.

Lin HY, Tang HY, Davis FB, Davis PJ. 2011b. Resveratrol and apoptosis. Ann N Y Acad Sci 1215:79–88.

Martin S, Phillips DC, Szekely-Szucs K, Elghazi L, Desmots F, Houghton JA. 2005. Cyclooxygenase-2 inhibition sensitizes human colon carcinoma cells to TRAIL-induced apoptosis through clustering of DR5 and concentrating death-inducing signaling complex components into ceramide-enriched caveolae. Cancer Res 65:11447–11458.

Mishra S, Raz A, Murphy LJ. 2004. Insulin-like growth factor binding protein-3 interacts with autocrine motility factor/phosphoglucoseisomerase (AMF/PGI) and inhibits the AMF/PGI function. Cancer Res 64:2516–2522.

Morrison J, Swanton A, Collins S, Kehoe S. 2007. Chemotherapy versus surgery for initial treatment in advanced ovarian epithelial cancer. Cochrane Database Syst Rev 17:CD005343.

Nickerson JA, Blencowe BJ, Penman S. 1995. The architectural organization of nuclear metabolism. Int Rev Cytol 162:67–123.

Oskouian B, Saba JD. 2010. Cancer treatment strategies targeting sphingolipid metabolism. Adv Exp Med Biol 688:185–205.

Parfenova H, Eidson TH, Leffler CW. 1997. Upregulation of COX-2 in cerebral microvascular endothelial cells by smooth muscle cell signals. Am J Physiol 273:C277–C288.

Parfenova H, Parfenov VN, Shlopov BV, Levine V, Falkos S, Pourcyrous M, Leffler CW. 2001. Dynamics of nuclear localization sites for COX-2 in vascular endothelial cells. Am J Physiol Cell Physiol 281:C166–C178.

Patel R, Attur MG, Dave M, Abramson SB, Amin AR. 1999. Regulation of cytosolic COX-2 and prostaglandin E2 production by nitric oxide in activated murine macrophages. J Immunol 162:4191–4197.

Pederson T. 1998. Thinking about a nuclear matrix. J Mol Biol 277:147–159.

Perry DK, Kolesnick RN. 2003. Ceramide and sphingosine 1-phosphate in anti-cancer therapies. Cancer Treat Res 115:345–354.

Ramer R, Weinzierl U, Schwind B, Brune K, Hinz B. 2003. Ceramide is involved in R(+)-methanandamide-induced cyclooxygenase-2 expression in human neuroglioma cells. Mol Pharmacol 64:1189–1198.

Roy S, Nicholson DW. 2000. Cross-talk in cell death signaling. J Exp Med 192: F21–F25.

Rüegg C, Zaric J, Stupp R. 2003. Non-steroidal anti-inflammatory drugs and COX-2 inhibitors as anti-cancer therapeutics: Hypes, hopes and reality. Ann Med 35:476–487.

Scarlatti F, Sala G, Somenzi G, Signorelli P, Sacchi N, Ghidoni R. 2003. Resveratrol induces growth inhibition and apoptosis in metastatic breast cancer cells via de novo ceramide signaling. FASEB J 17:2339–2341.

Sexton DW, Al-Rabia M, Blaylock MG, Walsh GM. 2004. Phagocytosis of apoptotic eosinophils but not neutrophils by bronchial epithelial cells. Clin Exp Allergy 34:1514–1524.

Shih A, Davis FB, Lin HY, Davis PJ. 2002. Resveratrol induces apoptosis in thyroid cancer cell lines via a MAPK- and p53-dependent mechanism. J Clin Endocrinol Metab 87:1223–1232.

Subbaramaiah K, Chung WJ, Dannenberg AJ. 1998. Ceramide regulates the transcription of cyclooxygenase-2. Evidence for involvement of extracellular signal-regulated kinase/c-Jun N-terminal kinase and p38 mitogen-activated protein kinase pathways. J Biol Chem 273:32943–32949.

Subbaramaiah K, Hart JC, Norton L, Dannenberg AJ. 2000. Microtubule-interfering agents stimulate the transcription of cyclooxygenase-2. Evidence for involvement of ERK1/2 and p38 mitogen-activated protein kinase pathways. J Biol Chem 275:14838–14845.

Swamy MV, Herzog CR, Rao CV. 2003. Inhibition of COX-2 in colon cancer cell lines by celecoxib increases the nuclear localization of active p53. Cancer Res 63:5239–5242.

Tang HY, Lin HY, Zhang S, Davis FB, Davis PJ. 2004. Thyroid hormone causes mitogen-activated protein kinase-dependent phosphorylation of the nuclear estrogen receptor. Endocrinology 145:3265–3272.

Tang HY, Shih A, Cao HJ, Davis FB, Davis PJ, Lin HY. 2006. Resveratrol-induced cyclooxygenase-2 facilitates p53-dependent apoptosis in human breast cancer cells. Mol Cancer Ther 5:2034–2042.

Trifan OC, Smith RM, Thompson BD, Hla T. 1999. Overexpression of cyclooxygenase-2 induces cell cycle arrest. Evidence for a prostaglandin-independent mechanism. J Biol Chem 274:34141–34147.

Van der Donk WA, Tsai AL, Kulmacz RJ. 2002. The cyclooxygenase reaction mechanism. Biochemistry 41:15451–15458.

Williams JL, Nath N, Chen J, Hundley TR, Gao J, Kopelovich L, Kashfi K, Rigas B. 2003. Growth inhibition of human colon cancer cells by nitric oxide (NO)-donating aspirin is associated with cyclooxygenase-2 induction and beta-catenin/T-cell factor signaling, nuclear factor-kappaB, and NO synthase 2 inhibition: Implications for chemoprevention. Cancer Res 63:7613–7618.

Xu XM, Sansores-Garcia L, Chen XM, Matijevic-Aleksic N, Du M, Wu KK. 1999. Suppression of inducible cyclooxygenase 2 gene transcription by aspirin and sodium salicylate. Proc Natl Acad Sci USA 96:5292–5297.

Yao M, Lam EC, Kelly CR, Zhou W, Wolfe MM. 2004. Cyclooxygenase-2 selective inhibition with NS-398 suppresses proliferation and invasiveness and delays liver metastasis in colorectal cancer. Br J Cancer 90:712–719.

Zahner G, Wolf G, Ayoub M, Reinking R, Panzer U, Shankland SJ, Stahl RA. 2002. Cyclooxygenase-2 overexpression inhibits platelet-derived growth factor-induced mesangial cell proliferation through induction of the tumor suppressor gene p53 and the cyclin-dependent kinase inhibitors p21waf-1/cip-1 and p27kip-1. J Biol Chem 277:9763–9771.

Zhao S, Yang YN, Song JG. 2004. Ceramide induces caspase-dependent and -independent apoptosis in A-431 cells. J Cell Physiol 199:47–56.